We are IntechOpen,
the world's leading publisher of
Open Access books
Built by scientists, for scientists

6,900
Open access books available

185,000
International authors and editors

200M
Downloads

154
Countries delivered to

Our authors are among the

TOP 1%
most cited scientists

12.2%
Contributors from top 500 universities

BOOK CITATION INDEX
CLARIVATE ANALYTICS
INDEXED

WEB OF SCIENCE™

Selection of our books indexed in the Book Citation Index
in Web of Science™ Core Collection (BKCI)

Interested in publishing with us?
Contact book.department@intechopen.com

Numbers displayed above are based on latest data collected.
For more information visit www.intechopen.com

Coherent Multilook Radar Detection for Targets in KK-Distributed Clutter

Graham V. Weinberg
Electronic Warfare and Radar Division
Defence Science and Technology Organisation (DSTO)
Australia

1. Introduction

1.1 The problem

This Chapter examines the problem of coherent multilook radar detection of targets in the sea from an airborne maritime surveillance platform. The radar of interest operates at high resolution, and at a high grazing angle, with frequency in X-Band, and is fully polarised. Typically, such surveillance radars are searching for small targets, such as fishing boats or submarine periscopes. When a radar transmits signals toward a potential target, the returned signal is distorted by a number of sources. The signal will be affected by thermal noise in the radar. Atmospheric conditions will also distort the signal. In a maritime surveillance context, backscatter from the rough sea surface will result in what is known as clutter returns Levanon (1988). In most cases, the first two sources of interference can be modelled by Gaussian processes Gini et al (1998). However, the sea clutter distribution is much more complex to model. Much research has consequently been dedicated to modelling sea clutter returns. Once a suitable clutter model has been proposed and validated, detection schemes can be designed using statistical methodology. This Chapter will construct radar detection schemes for a modern clutter model used for the scenario of interest. Before introducing this, a synopsis of clutter models is provided. Useful references on radar include Levanon (1988); Mahafza (1998); Peebles (1998); Stimson (1998). For statistical hypothesis testing, consult Beaumont (1980). For a detailed description of statistical and probability methods employed here, consult Durrett (1996). A useful reference on statistical distributions is Evans et al (2000).

1.2 Historical perspective

In earlier low resolution radar systems, sea clutter returns were found to be well modelled by a Rayleigh distribution for amplitude, with the exception of the case of low grazing angle scanning Shnidman (1999). As technology improved, and allowed the development of higher resolution radars, it was found that the Rayleigh assumption was no longer valid. As far back as 1967 it was found that data taken from a high resolution radar, operating at X-band with vertical polarization and a 0.002 μ second pulse, and at a grazing angle of 4.7°, deviated from the Rayleigh assumption significantly Trunk and George (1970). The major reason for the failure in the Rayleigh assumption is that the higher the radar's resolution, the smaller the resolution cells, and the corresponding clutter densities have greater tails than the zero mean Gaussian clutter models investigated by Marcum and Swerling Trunk and George (1970).

Within small resolution cells the clutter has been observed to consist of a series of discrete spikes, or high intensity returns, that vary in time. As is also reported in Trunk and George (1970), failure to alter the clutter model for high resolution radar results in an increased incidence of false alarms, which can seriously undermine a radar's performance. Hence it became critical to develop new models for high resolution radar sea clutter.

Sea clutter return statistics have also been found to have a complex dependence on a given radar's operating characteristics. In particular, it has been found that such statistics depend on the radar's operating mode, grazing angle and background operating environment. The clutter returns can vary significantly with grazing angle: the critical grazing angle $\theta_c = \frac{\lambda}{4\pi\sigma_h}$ divides the set of grazing angles into a "high" and "low" class. Here λ is the wavelength and σ_h is the root mean squared surface height deviation above average height Skolnik (2008). Clutter returns vary significantly over the partition of grazing angles by this threshold. At a low grazing angle, sea clutter returns are subjected to shadowing, ducting and multipath propogation Dong (2006); Skolnik (2008). By contrast, at higher grazing angles, the returns are affected by Bragg scattering from rough surface and scattering from whitecaps Dong (2006). It was reported in Crombie (1955) that at high frequency, wavelength scattering seemed to arise due to a resonant interaction with sea waves with one half of the incident wavelength. Such phenomenon is referred to as Bragg scattering. Whitecaps refer to the visible appearance of whitecaps in the sea surface as waves break Ward et al (2006). Wind speed affects the sea state, which in turn has a significant effect on clutter Skolnik (2008). The radar's polarization also has been found to affect the behaviour of clutter returns, with increased spikiness with horizontal polarization Dong (2006). Thus it is clear that adequate models for sea clutter backscattering must account for such phenomena as described above, and need to model the complex nature of true sea clutter returns.
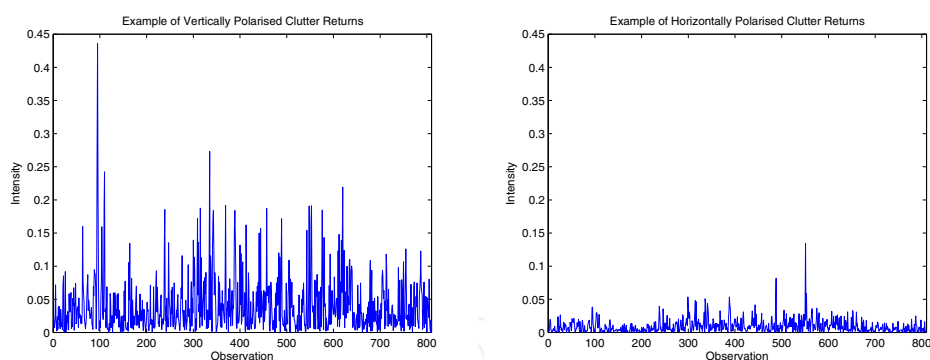

Fig. 1. Examples of real high grazing angle clutter. The left plot shows vertically polarized clutter, while the right is for horizontally polarization. All measurements are in intensity.

Figure 1 contains examples of real sea clutter returns, in the intensity domain, showing the changes in clutter as the radar's polarization is switched from vertical to horizontal, on a pulse to pulse basis. Both these examples of clutter have been obtained during a trial conducted by DSTO in the Southern Ocean using Ingara, an X-band fully polarized airborne radar Stacy et al (2003). The grazing angle for the clutter shown was $38.7°$. This has been taken from a range profile in data set run3468 at an azimuth angle of $225°$. Further details can be found in Stacy et al (2003), and will be provided with the numerical analysis to follow.

Earlier solutions to the inadequacy of the Rayleigh model include the Log-Normal Distribution, which was used for low grazing angles ($\theta \leq 5°$)

Trunk and George (1970), and the Weibull Distribution Schleher (1976). As reported in the latter, the Weibull model was found to be a close fit to high resolution radar sea clutter returns with a grazing angle $1° \leq \theta \leq 30°$. An attractive feature of the Weibull model is that it encompasses the two previous classical models of Rayleigh and Log-Normal.

However, it was found that the Weibull model was still insufficient because it did not take into account the complex nature of clutter. In fact, this model had been developed on the basis of empirical studies of clutter and not including any real physical understanding of the nature of sea clutter. Further investigation of high resolution sea clutter showed that time plots for an individual range cell demonstrated a fast pulse to pulse fluctuation. There was also an underlying slow modulation of the fast fluctuations. Presence of fast fluctuations and decorrelation with frequency agility implies there are many scatterers contributing to the resultant echo within each illumination patch. Hence an appropriate statistical model of clutter was needed to accommodate this phenomenon.

1.3 The K-Distribution

The K-Distribution was introduced in an attempt to model the phenomena described in the previous subsection. This model has a physical interpretation as well as a theoretical justification. This distribution models the observed fast fluctuations of clutter using a conditional Rayleigh distribution, while the underlying modulation is modelled through a Gamma distribution. Such a process can be described as a modulated Gaussian process. The short term or fast fluctuation is referred to as the speckle component, while the modulation or slow varying component is called the texture. The modern formulation of the K-Distribution can be traced back to Ward (1981), who arrived at it by considering high resolution sea clutter returns as a product of two independent random variables. One component has a short correlation time and is decorrelated by frequency agility (Rayleigh component referred to above). The other component has a long correlation time and models the underlying modulation or sea swell component (the Gamma distributed component).

The first appearance of the K-Distribution, applied to modelling radar clutter returns, is Jakeman and Pusey (1976). In the latter a mathematical model was developed for non-Rayleigh clutter, under the assumption that the illuminated area of the sea surface can be seen as a finite number of discrete scatterers. Each scatterer is assumed to give randomly phased contributions of the fluctuating amplitude in the radar's far field. The K-Distribution allowed explicit dependence on the illuminated area. In addition to this theoretical development, Jakeman and Pusey (1977) validated the K-Distribution as a model for X-band sea clutter taken from a coastal cliff site in England.

We now introduce the K-Distribution mathematically. The reference Ward et al (2006) is particularly useful in deriving K-Distribution properties.

The K-Distribution $X = [X_1, X_2]^T$ is defined, in the complex domain, as a bivariate random variable through the product

$$X = \sqrt{\frac{2\tau}{\pi}} X_{IQ}, \tag{1}$$

where $\tau = \tau(\mu, \nu)$ is a Gamma random variable with density

$$f_\tau(t) = \frac{1}{\Gamma(\nu)} \left(\frac{\nu}{\mu}\right)^\nu t^{\nu-1} e^{-\frac{\nu t}{\mu}}, \tag{2}$$

for $t \geq 0$, and $\mathbf{X}_{IQ}$ is a bivariate Gaussian random variable, with mean the 2×1 zero vector $\mathbf{0}$, covariance matrix the 2×2 identity matrix I_2 and density

$$f_{\mathbf{X}_{IQ}}(\mathbf{x}) = \frac{1}{2\pi} e^{-\frac{1}{2}\mathbf{x}^T\mathbf{x}}, \tag{3}$$

where $\mathbf{x}^T$ is the transpose of $\mathbf{x}$. The two components of $\mathbf{X}_{IQ}$ represent the in-phase and quadrature elements of the complex clutter return sampled by the radar. The Gamma distribution (2) has two free variables μ and ν. The former variable is an intermediate scale parameter, while ν is called a shape parameter. The $\sqrt{\tau}$ component in (1) is the slow varying component, while the Gaussian element is the fast varying component.

The representation (1) is convenient mathematically, from a signal processing point of view, when considering targets embedded in K-Distributed clutter and Gaussian noise. This is because, under the assumption of independent clutter and noise components in the return, we can use statistical conditioning on τ to combine these into one Gaussian component. This facilitates the analysis considerably: see Conte et al (1995); Farina et al (1995) for examples of this.

The amplitude of $\mathbf{X}$ is

$$K := |\mathbf{X}| = \sqrt{\frac{2\tau}{\pi}}|\mathbf{X}_{IQ}| = \sqrt{\frac{2\tau}{\pi}}R, \tag{4}$$

where the norm $|\cdot|$ in (4) is the standard Euclidean norm on vectors and $R := |\mathbf{X}_{IQ}|$.

The density of (4) can be derived by applying statistical conditioning; see Durrett (1996). In particular, by conditioning on the variable τ,

$$f_K(t) = \int_0^\infty f_{K|\tau}(t|\eta) f_\tau(\eta) d\eta. \tag{5}$$

With a considerable amount of analysis, it can be shown that

$$f_K(t) = \frac{2c}{\Gamma(\nu)} \left(\frac{ct}{2}\right)^\nu K_{\nu-1}(ct), \tag{6}$$

where $c = \sqrt{\frac{\pi\nu}{\mu}}$, giving the density function of the K-Distribution's amplitude. The parameter ν, which arises from the underlying Gamma Distribution, is referred to as the K-Distribution's shape parameter, while c is called the scale parameter. The shape parameter ν governs the tail of the K-Distribution's density, and it has been found that small values of ν represent more spiky clutter Crisp et al (2009). Larger values of ν produce backscattering that is closer to Rayleigh in distribution. As reported in Crisp et al (2009), ν around 0.1 corresponds to very spiky clutter, while ν near 20 produces approximate Rayleigh clutter.

The cumulative distribution function of the K-Distribution can be obtained by integrating (6) over the interval $[0, t]$. It can be shown that

$$F_K(t) = \mathbf{P}(K \leq t) = 1 - \frac{(ct)^\nu K_\nu(ct)}{2^{\nu-1}\Gamma(\nu)}. \tag{7}$$

As reported in Dong (2006), the first two moments of K are given by

$$\mathbf{E}(K) = \frac{\sqrt{\pi}\Gamma(\nu + \frac{1}{2})}{c\Gamma(\nu)} \text{ and } \mathbf{E}(K^2) = \frac{4\nu}{c^2}, \tag{8}$$

and consequently the K-Distribution's variance can be obtained as

$$\text{Var}(K) = \mathbf{E}(K^2) - [\mathbf{E}(K)]^2 = \frac{1}{c^2}\left[4\nu - \frac{\pi\Gamma^2(\nu+0.5)}{\Gamma^2(\nu)}\right]. \tag{9}$$

1.4 Modifying the K-Distribution: The KA-Distribution

As remarked in the previous subsections, the K-Distribution was introduced in an attempt to reflect the complex nature of sea clutter backscattering of high resolution radars. However, it has been found that horizontally polarised data tends to be spikier than that obtained from a vertically polarized radar. In the latter, the K-Distribution is a suitable model, but in the former, there is a deviation in the distribution's tail region. Hence, this resulted in the search for a new model that incorporated such deviations in the distribution's fit.

A major step toward this objective was the introduction of the KA-Distribution in Middleton (1999). In this model, the fast varying component is still Rayleigh Distributed, but it is conditioned on the number of spikes in each range cell. The latter is assumed to follow a Poisson Distribution. The slow varying component is still Gamma Distributed, which is the local intensity of Bragg/whitecap scatterers. Mathematically, the KA-Distribution is defined in an identical formulation to (5). Specifically, its density is given by the integral

$$f_{KA}(x) = \int_0^\infty f_{KA|\tau}(x|t)f_\tau(t)dt, \tag{10}$$

where τ has a Gamma Distribution with parameters ν and $\mu = \sigma_{bw}$ (refer to (2)). The conditional distribution $KA|\tau$ has density

$$f_{KA|\tau}(x|t) = \sum_{n=0}^\infty \frac{2x}{t+\sigma_n+n\sigma_{sp}}e^{-\left(\frac{x^2}{t+\sigma_n+n\sigma_{sp}}\right)}\rho(n), \tag{11}$$

where $\rho(n) = \frac{e^{-\bar{N}}\bar{N}^n}{n!}$ is the Poisson probability that a range cell contains n spikes. In (11), σ_n is the mean noise intensity, σ_{sp} is the spike intensity, σ_{bw} is the mean Bragg/whitecap intensity and $\bar{N}$ is the mean number of spikes in each range cell Dong (2006). As also pointed out in the latter, the noise, spikes and Bragg/whitecap scatterers are all assumed to be mutually uncorrelated. The expression (11) is the law of total probability applied over all possible number of spikes in range cells.

The KA-Distribution was also investigated in Ward and Tough (2002) and Watts et al (2005), and was shown to improve the fit of sea clutter in the distribution's tail region. Further validation of the KA-Distribution's fit to spiky sea clutter is given in Valeyrie et al (2009) using airborne radar records in rough sea states. Unfortunately, there is no closed form expression for the density of the KA-Distribution.

1.5 The KK-Distribution

The KK-Distribution was proposed in Dong (2006) as an alternative to the KA-Distribution. This Distribution assumes both the Bragg/whitecap scatterers and spikes are K-Distributed. The overall clutter distribution is defined as a mixture of the two: namely, a weighted sum of densities of the respective components Dong (2006). This formuation leads to a closed form

for the density, in the amplitude domain, in terms of K-Distribution densities, and statistical properties can be determined via linearity of the density, as will be demonstrated below.

In particular, for a fixed parameter $k \in [0, 1]$, the amplitude density of the KK-Distribution is defined as the mixture

$$f_{KK}(t) = (1 - k)f_{K_1}(t; \sigma, \nu) + kf_{K_2}(t; \sigma_{sp}, \nu_{sp}), \tag{12}$$

where each f_{K_j} is a K-Distribution with parameters (σ, ν) and (σ_{sp}, ν_{sp}) respectively. The first K-Distribution density in (12) represents the Bragg and whitecap scatterers in the model. The second K-Distribution in (12) represents the spike component of the clutter.

The restricted range of values for k ensures (12) preserves the features of a probability density. As reported in Dong (2006), it has been found empirically that we may assume $\nu = \nu_{sp}$, and so selection of k, ν_{sp} and $\rho := \frac{\sigma_{sp}}{\sigma}$ determines the spike component. Throughout we will use the notation $c_1 = \sigma$ and $c_2 = \sigma_{sp}$ for the two scale parameters.

Comparison of this model to high resolution radar sea clutter has been recorded in Dong (2006), where it is shown the KK-Distribution provides a better fit to the upper tail region of the empirical distribution than the K- and KA-Distributions. The KK-Distribution's validity is also supported by the analysis of trials data in Rosenberg et al (2010), who also extend the model to include multiple looks and thermal noise.

The moments of the KK-Distribution can be obtained from those of the K; in particular, if we let KK be a random variable with the density (12), it follows that

$$\mathbf{E}(KK) = (1 - k)\mathbf{E}(K_1) + k\mathbf{E}(K_2) = \frac{\sqrt{\pi}\Gamma(\nu)}{\Gamma(\nu + \frac{1}{2})}\left(\frac{1 - k}{c_1} + \frac{k}{c_2}\right), \tag{13}$$

where we have applied (8) for two K-Distributions with common shape parameter ν and scale parameters c_1 and c_2 respectively. The KK-Distribution's second moment can also be derived from (8): in particular, and under the same parameter values, we can show

$$\mathbf{E}(KK^2) = (1 - k)\mathbf{E}(K_1^2) + k\mathbf{E}(K_2^2) = 4\nu\left(\frac{1 - k}{c_1^2} + \frac{k}{c_2^2}\right). \tag{14}$$

We can use (13) and (14) to derive the KK-Distribution's variance. It is straightforward to derive

$$\mathrm{Var}(KK) = 4\nu\left(\frac{1 - k}{c_1^2} + \frac{k}{c_2^2}\right) - \frac{\pi\Gamma^2(\nu)}{\Gamma^2(\nu + \frac{1}{2})}\left(\frac{1 - k}{c_1} + \frac{k}{c_2}\right)^2. \tag{15}$$

The cumulative probability density function of the KK-Distribution can be obtained from the fact that

$$F_{KK}(t) = (1 - k)F_{K_1}(t) + kF_{K_2}(t)$$

$$= 1 - \frac{t^\nu}{2^{\nu-1}\Gamma(\nu)}\left((1 - k)K_\nu(c_1 t)c_1^\nu + kK_\nu(c_2 t)c_2^\nu\right), \tag{16}$$

where the parameter sets $\{c_1, \nu\}$ and $\{c_2, \nu\}$ are for the two K-Distributions K_1 and K_2 respectively.

1.6 Scope, assumptions and structure

This Chapter will be focused on multilook radar detection of targets embedded within KK-Distributed clutter. In order to do this, a number of assumptions will be made. Throughout, the thermal noise and Gaussian interference will be ignored. It will be assumed that the radar has the capability to determine the clutter parameters, so that these are known from the detection point of view. The clutter covariance matrix will also be assumed known, and furthermore, it will be assumed its inverse is semi-positive definite. It will be assumed that the normalised Doppler frequency (to be specified later) is also known. The Neyman-Pearson approach will be employed to construct detection schemes. The focus will be restricted to coherent radar detection.

Section 2 formulates the KK-Distribution as an intensity distribution of a complex spherically invariant random process. This enables the determination of the Neyman-Pearson optimal decision rule in Section 3. The generalised likelihood ratio test will be used to construct a suitable suboptimal decision rule, which assumes the target is constant on a scan to scan basis. Section 4 introduces the Ingara data briefly, and investigates receiver operating characteristics curves. These provide a means of gauging the performance of a detction scheme over varying signal to clutter strengths.

Throughout we will use $\mathbf{P}$ to denote probability, $\mathbf{E}$ to be expectation with respect to $\mathbf{P}$, and $X \stackrel{d}{=} Y$ will represent equivalence in distribution.

2. Coherent multilook detection

2.1 Spherically invariant random processes

Spherically Invariant Random Processes (SIRPs) Rangaswamy et al (1993); Wise (1978); Yao (1973) provide a general formulation of the joint density of a non-Gaussian random process, enabling the construction of densities for Neyman-Pearson detectors Beaumont (1980); Neyman and Pearson (1933).

Traditionally, a SIRP is introduced as a process whose finite order subprocesses, called Spherically Invariant Random Vectors (SIRVs), possess a specific density Conte and Longo (1987); Rangaswamy et al (1991). However, due to an equivalent formulation, we can specify SIRVs and SIRPs in a manner more intuitive to the modelling of radar returns as follows. Let $c = \{\varsigma_1, \varsigma_2, \ldots, \varsigma_N\}$ be the complex envelope of the clutter returns. Then this vector is called SIRV if it can be written in the compound-Gaussian formulation

$$c = S\mathcal{G}, \tag{17}$$

where the process $\mathcal{G} = (G_1, G_2, \ldots, G_N)^T$ is a zero mean complex Gaussian random vector, or multidimensional complex Gaussian process, and S is a nonnegative real valued univariate random variable with density f_S. The latter random variable is assumed to be independent of the former process. If such a decomposition exists for every $N \in \mathbb{N}$ the complex stochastic process $\{\varsigma_1, \varsigma_2, \ldots\}$ is called spherically invariant. For a comprehensive description of the modelling of clutter via SIRPs consult Conte and Longo (1987). What is clear from the formulation (17) is that, by conditioning on the random variable S, we can write down the density of c as a convolution. This will be shown explicitly in the analysis to follow.

2.2 General formulation

The detection decision problem is now formulated. We assume that we have a SIRP model for the clutter c as specified through the product formulation (17). Suppose the radar return is z, which is a complex $N \times 1$ vector. Then the coherent multilook detection problem can be cast in the form

$$H_0 : z = c \text{ against } H_1 : z = Rp + c, \tag{18}$$

where all complex vectors are $N \times 1$, and H_0 is the null hypothesis (return is just clutter) and H_1 is the alternative hypothesis (return is a mixture of signal and clutter). Statistical hypothesis testing is outlined in Beaumont (1980). Here, the vector p is the Doppler steering vector, whose components are given by $p(j) = e^{j2\pi i f_D T_s}$, for $j \in \{1, 2, \ldots, N\}$, where f_D is the target Doppler frequency and T_s is the radar pulse repetition interval. It will be assumed that this is completely known. The complex random variable R accounts for target characteristics, and $|R|$ is the target amplitude. Suppose the zero mean Gaussian process has covariance matrix $\text{Cov}(\mathcal{G}) = \mathbf{E}(\mathcal{G}\mathcal{G}^H) = \Sigma$. Since it is a covariance matrix, its inverse will exist. Recall that (since Σ^{-1} is also a covariance matrix), the inverse will be symmetric and positive definite. If we assume it is semi-definite positive, then we can apply a whitening filter approach to simplify the detection problem. Hence we suppose the Cholesky Factorisation exists for Σ^{-1}, so that there exists a matrix A such that $\Sigma^{-1} = A^H A$.

A SIRP is unaffected by a linear transformation Rangaswamy et al (1993). This means that applying a linear operator to the clutter process alters the complex Gaussian component, but the characteristic function of the SIRP is preserved. Hence in the literature, a whitening approach is often applied to the detection problem of interest. Note that, by applying the Cholesky factor matrix A to the statistical test, we can reformulate (18) in the statistically equivalent form

$$H_0 : r = n \text{ against } H_1 : r = Ru + n, \tag{19}$$

where $r = Az, n = Ac$ and $u = Ap$.

The transformed clutter process $n = SA\mathcal{G}$, and $A\mathcal{G}$ is still a multidimensional complex Gaussian process, with zero mean but covariance $\text{Cov}(A\mathcal{G}) = \mathbf{E}(A\mathcal{G}\mathcal{G}^H A^H) = A\Sigma A^H$.

Since $\Sigma^{-1} = A^H A$, it follows that $I_{N \times N} = \Sigma A^H A$, from which it is not difficult to deduce that $A = (A\Sigma A^H)A$. Let $B = A\Sigma A^H$, then note that $B^2 = B$, so that B is idempotent. Also, it follows that B must be invertible, since $det(B) = det(A)det(\Sigma)det(A^H)$ and $det(\Sigma) \neq 0$ and $det(\Sigma^{-1}) = det(A^H)det(A) \neq 0$. Thus it follows that B must be the $N \times N$ identity matrix. Consequently, we conclude that the transformed Gaussian process $A\mathcal{G}$ has zero mean and covariance matrix this identity matrix. Hence the clutter, conditioned on the variable S, is completely decorrelated through this linear transform.

We write this as $A\mathcal{G} \stackrel{d}{=} CN(\vec{0}, I_{N \times N})$. Observe that $n|S$ is still complex Gaussian with zero mean vector but covariance matrix $s^2 I_{N \times N}$, hence its density is

$$f_{n|S=s}(x) = \frac{1}{\pi^N s^{2N}} e^{-s^{-2}\|x\|^2}. \tag{20}$$

Hence by using conditional probability Durrett (1996)

$$f_{\boldsymbol{n}}(\boldsymbol{x}) = \int_0^\infty f_{\boldsymbol{n}|S=s}(\boldsymbol{x}) f_S(s) ds$$

$$= \int_0^\infty \frac{1}{\pi^N s^{2N}} e^{-s^{-2}\|\boldsymbol{x}\|^2} f_S(s) ds. \tag{21}$$

Hence if we define a function $h_N(p)$ by

$$h_N(p) = \int_0^\infty s^{-2N} e^{-s^{-2}p} f_S(s) ds, \tag{22}$$

then the clutter joint density can be written in the compact form

$$f_{\boldsymbol{n}}(\boldsymbol{x}) = \frac{1}{\pi^N} h_N(\|\boldsymbol{x}\|^2). \tag{23}$$

The function h_N defined in (22) is of paramount importance in SIRP theory, as all densities of interest are expressed in terms of it. It is thus called the characteristic function. Much of the literature is devoted to determining h_N and f_S pairs for particular desired clutter models Rangaswamy et al (1991; 1993).

Next we derive the marginal amplitude and intensity distributions of the complex clutter process $\boldsymbol{n}$, which are intimately related to the special function h_N. Let the kth element of $\boldsymbol{n}$ be n_k, so that $n_k = SA\boldsymbol{\mathcal{G}}_k$, where $\boldsymbol{\mathcal{G}}_k$ is the kth component of $\boldsymbol{\mathcal{G}}$, for $1 \leq k \leq N$. Then the complex Gaussian density of $A\boldsymbol{\mathcal{G}}_k$ is

$$f_{A\boldsymbol{\mathcal{G}}_k}(z) = \frac{1}{\pi} e^{-|z|^2}. \tag{24}$$

Hence, equivalently, $A\boldsymbol{\mathcal{G}}_k$ is a bivariate Gaussian process with zero mean and covariance matrix $\frac{1}{2} I_{2\times 2}$. Consequently, it follows that its amplitude $|A\boldsymbol{\mathcal{G}}_k|$ has a Rayleigh distribution with parameter $\frac{1}{\sqrt{2}}$. Hence, using the fact that S and $A\boldsymbol{\mathcal{G}}_k$ are independent, and the definition of the Rayleigh density, we can show that

$$f_{|n_k|}(t) = \int_0^\infty \frac{2t}{s^2} e^{-\frac{t^2}{s^2}} f_S(s) ds = 2t h_1(t^2), \tag{25}$$

yielding the marginal amplitude distribution for each k. Transforming to the intensity domain, it is not difficult to show

$$f_{|n_k|^2}(t) = \frac{1}{2} t^{-\frac{1}{2}} f_{|n_k|}(\sqrt{t}) = h_1(t), \tag{26}$$

also for each k.

The importance of the results (25) and (26) is that they indicate how an arbitrary distribution can be embedded within a SIRP model. The key to the determination of a relevant SIRP for a given detection problem is the specification of the random variable S through its density f_S. For a desired marginal distribution, we can form an integral equation using (26) and (22) with $N = 1$. The literature contains extensive discussion of this problem; in particular, Rangaswamy et al (1993) contains guidelines on performing this, as well as case studies for most desired marginal distributions.

2.3 The KK-SIRP

The key to constructing the KK-SIRP is to observe the fact that, since it is defined as a mixture in the amplitude domain, we can use the K-Distribution SIRP, which is well known. This is specified in Rangaswamy et al (1993). The following specifies the density of S for a K-Distribution:

Lemma 2.1. *The SIRP with nonnegative random variable S with density given by*

$$f_S(s) = \frac{\sqrt{2}c^{2\nu}}{\Gamma(\nu)} s^{2\nu-1} e^{-\frac{c^2 s^2}{4}}, \tag{27}$$

admits a K-Distribution, with parameters c and ν, as marginal amplitude distributions.

Extending this result to the KK-Distribution case is simple, as the following Lemma encapsulates:

Lemma 2.2. *The function*

$$f_S(s) = (1-k)f_{S_1}(s) + kf_{S_2}(s), \tag{28}$$

with $k \in [0,1]$ and each $f_{S_i}(s)$ given by (27) with parameters c_i and ν_i, is a well-defined density on the nonnegative real line. Furthermore, it admits a KK-Distribution with scale parameters c_i and shape parameters ν_i.

The proof of Lemma 2.2 is not difficult, and is hence omitted. It requires the application of Lemma 2.1, together with the following result:

Lemma 2.3. *For the SIRP generated by the density (28),*

$$h_N(u) = \frac{u^{\frac{nu-N}{2}}\zeta(\sqrt{u}; c_1, c_2, \nu, k)}{\Gamma(\nu)2^{1.5\nu+0.5N-1}}, \tag{29}$$

with ζ defined by

$$\zeta(u; c_1, c_2, \nu, N, k) = (1-k)c_1^{N+\nu}K_{N-\nu}(c_1 u) + kc_2^{N+\nu}K_{N-\nu}(c_2 u). \tag{30}$$

The proof of Lemma 2.3 involves simplification of the characteristic function (22), application of Lemma 2.1 and use of the corresponding properties of the K-Distribution SIRP Rangaswamy et al (1993).

3. Detector decision rules

Using the KK-SIRP formulated in the previous section, we can now derive the Neyman-Pearson optimal decision rules, including suboptimal approximations.

3.1 Optimal decision rule: constant target

It is useful to begin with the case of a fixed known target model, which means we assume that R is a fixed constant that is completely specified. This enables one to specify the exact form of the Neyman-Pearson optimal detector. Throughout, we will also assume the clutter parameters have been estimated by the radar system, so that they are completely known. It is also assumed that the clutter parameters are homogeneous within a range profile scan.

Under H_1, $\boldsymbol{r} = R\boldsymbol{u} + \boldsymbol{n}$, and conditioned on S, this is still complex Gaussian, with the same covariance as $\boldsymbol{n}$ (since $R\boldsymbol{u}$ is constant), but its mean is shifted by the vector $R\boldsymbol{u}$. Hence the density under H_1 is

$$f_{H_1}(\boldsymbol{r}) = \frac{1}{\pi^N} h_N(\|\boldsymbol{r} - R\boldsymbol{u}\|^2). \tag{31}$$

The Neyman-Pearson optimal detector is the ratio of the densities under H_1 and H_0 Beaumont (1980). The density under H_0 is given by (23), with an application of (29). Hence, combining these results, we get the likelihood function

$$L(\boldsymbol{r}) = \frac{h_N(|\boldsymbol{r} - R\boldsymbol{u}|^2)}{h_N(|\boldsymbol{r}|^2)}$$

$$= \left(\frac{|\boldsymbol{r} - R\boldsymbol{u}|}{|\boldsymbol{r}|} \right)^{\nu - N} \frac{\zeta(|\boldsymbol{r} - R\boldsymbol{u}|; c_1, c_2, \nu, N, k)}{\zeta(|\boldsymbol{r}|; c_1, c_2, \nu, N, k)}, \tag{32}$$

and the optimal decision rule is

$$L(\boldsymbol{r}) \underset{H_0}{\overset{H_1}{\gtrless}} \tau, \tag{33}$$

where τ is the detection threshold, which can be determined numerically from the false alarm probability. The notation $X \underset{H_0}{\overset{H_1}{\gtrless}} Y$ means that we reject H_0 if and only if $X > Y$. Hence for a radar return $\boldsymbol{r}$ we compare $L(\boldsymbol{r})$ to the threshold τ to make a decision on whether a target signature is present in the return.

In all reasonable practical applications, we will not have knowledge of R, and so we must extend this result to account for an unknown R. This is the subject of the next Subsection.

3.2 Generalised likelihood ratio test

In a real application, the target is unknown and hence R must be estimated. If we assume R is unknown but constant from scan to scan, the Generalised Likelihood Ratio Test is used to first estimate this parameter, and then apply the estimate to the test (33). The methodology of GLRT is described in Barnard and Khan (2004); Conte et al (1995). We essentially produce a suboptimal detector for the case of an unknown target, based upon the optimal decision rule formulated for a completely known target model.

We call this estimate $\hat{R}$, which is taken to be the maximum likelihood estimator Beaumont (1980). It is chosen to minimise the quantity $\|\boldsymbol{r} - R\boldsymbol{u}\|^2$. This is because, in view of the density (31) and the definition of h_N in (22), maximising the density with respect to R is equivalent to minimisation of this quantity.

By applying a simple expansion, we can show

$$\|\boldsymbol{r} - R\boldsymbol{u}\|^2 = \|\boldsymbol{r}\|^2 + |R|^2 \|\boldsymbol{u}\|^2 - 2\Re(\bar{R}\boldsymbol{u}^H \boldsymbol{r}), \tag{34}$$

where $\Re(z)$ is the real part of the complex number z. Recalling the proof of the Cauchy-Schwarz inequality (see Kreyszig (1978) for example), this is minimised with the choice $\hat{R} = \frac{\boldsymbol{u}^H \boldsymbol{r}}{\|\boldsymbol{u}\|^2}$. Substituting this in (34) shows that

$$\min_R \|\boldsymbol{r} - R\boldsymbol{u}\|^2 = \|\boldsymbol{r} - \hat{R}\boldsymbol{u}\|^2 = \|\boldsymbol{r}\|^2 - \frac{|\boldsymbol{u}^H \boldsymbol{r}|^2}{\|\boldsymbol{u}\|^2}. \tag{35}$$

An application of (35) to (33) results in the GLRT.

4. Numerical analysis of detectors

4.1 The Ingara data

Before proceeding with an analysis of the optimal and suboptimal detectors, the Ingara data is discussed briefly. This sea clutter set was collected by DSTO, using their radar testbed called Ingara. This is an X-Band fully polarised radar. The 2004 trial used to collect the data was located in the Southern Ocean, roughly 100km south of Port Lincoln in South Australia. Details of this trial, the Ingara radar, and data analysis of the sea clutter can be found in Crisp et al (2009); Dong (2006); Stacy et al (2003; 2005).

The radar operated in a circular spotlight mode, so that the same patch of sea surface was viewed at different azimuth angles. The radar used a centre frequency of 10.1 GHz, with 20 μs pulse width. Additionally, the radar operated at an altitude of 2314m for a nominal incidence angle of $50°$, and at 1353m for $70°$ incidence angle. The trial collected data at incidence angles varying from $40°$ to $80°$, on 8 different days over an 18 day period. As in Dong (2006), we focus on data from two particular flight test runs. These correspond to run34683 and run34690, which were collected on 16 August 2004 between 10:52am and 11:27am local time Dong (2006). Dataset run34683 was obtained at an incidence angle of $51.5°$, while run34690 was at $67.2°$. In terms of grazing angles, these correspond to $38.7°$ and $22.8°$ respectively. Each of these datasets were also processed in blocks to cover azimuth angle spans of $5°$ over the full $360°$ range. Roughly 900 pulses were used, and 1024 range compressed samples for each pulse were produced, at a range resolution of 0.75m. In Dong (2006) parameter estimates for the data sets run34683 and run34690 are given, enabling the fitting of the K- and KK-Distributions to this data. This will be employed in the numerical analysis to follow.

As reported in Dong (2006), the radar is facing upwind at approximately $227°$ azimuth, which is the point of strongest clutter. Downwind is at approximately $47°$, which is the point where the clutter is weakest. Crosswind directions are encountered at $137°$ and $317°$ approximately.

4.2 Target model and SCR

Since the Ingara clutter does not contain a target, an artificial model is used to produce the receiver operating characteristics (ROC) curves. These curves plot the probability of detection against the signal to clutter ratio (SCR). It hence indicates the performance of a detector relative to varying signal strengths in the clutter model.

Throughout, a Swerling 1 target model is used Levanon (1988). This is equivalent to assuming that the in-phase and quadrature components of the signal return are complex Gaussian in distribution. For the problem under investigation, the SCR is given by

$$SCR = \frac{\mathbf{E}(|R|^2)\,|\boldsymbol{u}|^2}{\mathbf{E}(S^2)N},$$

(36)

and it is not difficult to show that

$$\mathbf{E}(S^2) = 4\nu\left[\frac{1-k}{c_1^2} + \frac{k}{c_2^2}\right].$$

(37)

Hence, assuming for the Swerling 1 target model, $\mathbf{E}|R|^2 = 2\sigma^2$, an application of this to (36) yields

$$SCR = \frac{\sigma^2 |\boldsymbol{u}|^2}{2N\nu \left[\frac{1-k}{c_1^2} + \frac{k}{c_2^2}\right]}. \tag{38}$$

The ROC curves to follow are produced by determining the parameter σ^2, for a given SCR, using (38).

4.3 Receiver operating characteristics curves

Four examples of detector performance are provided. In all cases, the ROC curves have been produced using Monte Carlo simulations, with approximately 10^5 runs. Each simulation is for the case of a false alarm probability of 10^{-6}. The SCR is varied from -10 to 30 dB. Each ROC curve shows the performance of the optimal decision rule (33), the GLRT decision rule using (35) to estimate the target strength and the performance of the whitening matched filter. The latter is the optimal detector for targets in Gaussian distributed clutter, and can be used as a suboptimal decision rule. For a return $\boldsymbol{r}$, it is given by

$$M(\boldsymbol{r}) = \left|\boldsymbol{u}^H \boldsymbol{r}\right|^2, \tag{39}$$

where $\boldsymbol{u}^H$ is the Hermitian transpose. Although the decision rule (33) is dependent on the target parameters, and so is not useful in practice, it is used here to gauge the performance of the two suboptimal decision rules.

Each simulation uses parameters estimated from a specific Ingara data set. The clutter used for each ROC curve is produced by simulating a zero mean complex Gaussian process whose covariance matrix is specified, and so is not regressed from real data. This is then multiplied by a simulation of S with density (28) to produce a simulation of the SIRP.

4.3.1 Examples for horizontal polarisation

Two cases are considered for the horizontally polarised case. The first is for the scenario where the KK-Distributed clutter takes parameters $c_1 = 1, c_2 = 3.27, \nu = 4.158$, and $k = 0.01$. These parameters have been selected based upon the estimates for the clutter set run34683 described above, and with parameters estimated based upon the results in Dong (2006). For this case, the azimuth angle is $225°$, which is nearly upwind. The number of looks is $N = 30$, and the clutter covariance matrix has been produced using simulated variables. Additionally, for this example, the normalised Doppler frequency is generated from $f_D = 1$ and $T_s = 0.5$. The corresponding ROC curve can be found in Figure 2 (left subplot). This shows the optimal detector and GLRT detector matching very closely. Increasing the number of Monte Carlo samples improves the plot, but takes long periods to generate. The main feature one can observe from this plot is that the GLRT performs very well in this case, and certainly outperfoms the WMF.

The second example considered is illustrated also in Figure 2 (right subplot). This is for the case where the KK-Distribution has parameters $c_1 = 8, c_2 = 46.16, \nu = 4.684, k = 0.01, f_D = 0.8, T_s = 0.5$, with the number of looks $N = 20$. The clutter parameters have been estimated from data set run34683 with azimuth angle $190°$. The clutter covariance matrix was generated with random Gaussian numbers. The plot shows the same phenomenon as for the previous example.
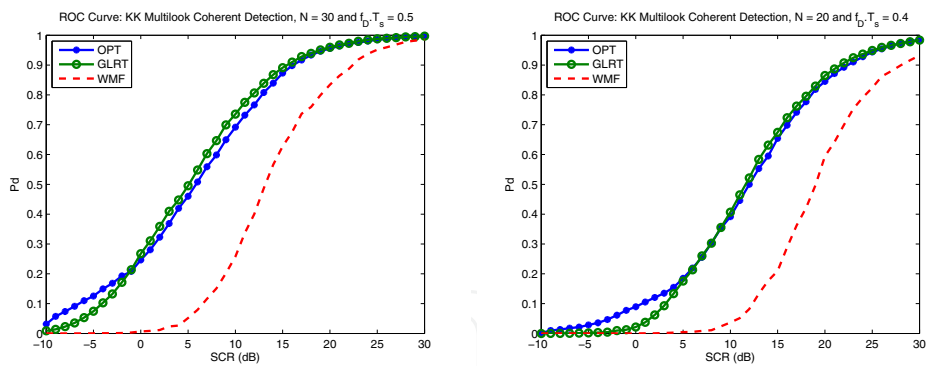
Fig. 2. ROC curves, Horizontal polarisation, clutter set run34683, azimuth angles $225°$ (left plot) and $190°$ (right plot). OPT corresponds to (33), GLRT to the suboptimal rule using (35) and WMF is (39).

4.3.2 Examples for vertical polarisation

The vertically polarised case is illustrated in Figure 3. The first subplot is for the scenario where $c_1 = 25, c_2 = 26.5, \nu = 8.315, k = 0.01, f_d = 100$ and $T_s = 0.5$. $N = 10$ looks have been used. These correspond to run34690, with azimuth angle $45°$, which is almost down wind in direction. For this case, it is interesting to note that the GLRT and WMF match very closely. It is only under increased magnification that it can be shown the GLRT is marginally better. The same phenomenon is also demonstrated for the case where $c_1 = c_2 = 35, \nu = 12.394, f_D = 10$ and $T_s = 0.5$, with $N = 5$ looks. This is illustrated in Figure 3 (right subplot). This example is based upon the clutter set run34690, at an azimuth angle of $315°$, which is approximately crosswind.
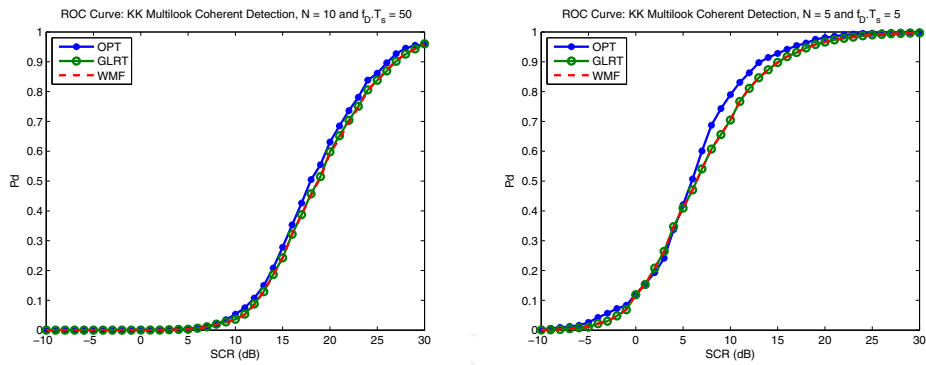
Fig. 3. ROC curves corresponding to the vertically polarised case, for clutter set run34690, azimuth angles $45°$ (left plot) and $315°$ (right plot). Here, the GLRT and WMF match almost exactly, suggesting the WMF is a suitable suboptimal decision rule.

4.3.3 Analysis of detectors

Examination of ROC curves for other Ingara clutter sets showed roughly the same results. For the vertically polarised channel, the WMF was a valid approximation to the GLRT, and is preferable because it does not require knowledge of clutter parameters. This result can be explained from the fact that the vertically polarised clutter is not as spiky as the horizontally polarised case, and the Gaussian distribution is the limit of a K-Distribution as the shape parameter increases. The latter results in less spiky clutter. For the horizontally polarised case, the clutter is spikier and so the GLRT is much better.

5. Conclusions and further research

The KK-Distribution was embedded within a SIRP in the complex domain, so that the Neyman-Pearson optimal detector could be constructed for multilook detection. A GLRT solution was then constructed, and this, together with the WMF suboptimal decision rule, were compared using ROC curves. These ROC curves were generated using clutter parameter estimates based upon the Ingara data set. For the horizontally polarised case, it was shown that the GLRT produced a very good probability of detection for a Swerling 1 target model. In the case of vertically polarised returns, the WMF often matched the performance of the GLRT. Hence, in such cases, the WMF can be used as a simpler suboptimal detector.

Further work will be spent on trying to find suboptimal decision rules based upon simplification of the GLRT solution. Additionally, performance analysis of detectors for other target models will be undertaken.

6. References

Barnard, T. J. and Khan, F. (2004). Statistical Normalization of Spherically Invariant Non-Gaussian Clutter. *IEEE J. Ocean. Eng.* Vol. 29, 303-309.

Beaumont, G. P. (1980). *Intermediate Mathematical Statistics*, Chapman and Hall, London.

Conte, E. and Longo, M. (1987). Characterisation of radar clutter as a spherically invariant random process. *Proceed. IEEE* Vol. 134 F, 191-197.

Conte, E., Lops, M. and Ricci, G. (1995). Asymptotically Optimum Radar Detection in Compound Gaussian Clutter. *IEEE Trans. Aero. Elec. Sys.* Vol. 31, 617-625.

Crisp, D. J., Rosenberg, L., Stacy, N. J. and Dong, Y. (2009). Modelling X-Band Sea Clutter with the K-Distribution: Shape Parameter Variation, *IEEE Conf. Surveillance for a Safer World*, Bordeaux, France.

Crombie, D. (1955). Doppler Spectrum of Sea Echo at 13.56Mc/s. *Nature* Vol. 175, 681-682.

Dong, Y. (2006). Distribution of X-Band High Resolution and High Grazing Angle Sea Clutter. *DSTO Research Report* DSTO-RR-0316.

Durrett, R. (1996) *Probability: Theory and Examples, 2nd Edition*. Wadsworth, California.

Evans, M., Hastings, N. and Peacock, B.(2000). *Statistical Distributions, 3rd Edition*. Wiley, New York.

Farina, A., Gini, F., Greko, M. V. and Lombardo, P. (1995). Coherent Radar Detection of Targets Against a Combination of K-Distributed and Gaussian Clutter. *Proceed. IEEE Int. Radar, Conf.,* 83-88.

Gini, F., Greko, M. V., Farina, A. and Lombardo, P. (1998) Optimum and Mismatched Detection Against K-Distributed Plus Gaussian Clutter. *IEEE Trans. Aero. Elec. Sys.* Vol. 34, 860-876.

Jakeman, E. and Pusey, P. N. (1976). A model for Non-Rayleigh Sea Echo. *IEEE Trans. Antennas Prop.* Vol AP24, 806-814.

Jakeman, E. and Pusey, P. N. (1977). Statistics of Non-Rayleigh Sea Echo. *IEE Conf. Publ. 155* Radar 1977, 105-109.

Kreyszig, E. (1978). *Introductory Functional Analysis with Applications*. Wiley, New York.

Levanon, N. (1988). *Radar Principles*. Wiley, New York.

Mahafza, B. R.(1998). *Introduction to Radar Analysis*. CRC Press, Florida.

Middleton, D. (1999). New Physical-Statistical Methods and Models for Clutter and Reverberation: The KA-Distribution and Related Probability Structures. *IEEE J. Oceanic Eng.* Vol 24, 261-284.

Neyman, J. and Pearson, E. (1933). On the Problem of the Most Efficient Tests of Statistical Hypotheses. *Phil. Trans. Royal Soc. Lond.* Series A 231, 289-337.

Peebles, P. Z. (1998). *Radar Principles*. Wiley, New York.

Rangaswamy, M., Weiner, D. and Ozturk, A. (1991). Simulation of Correlated Non-Gaussian Interference for Radar Signal Detection, *Proceed. IEEE*, 148-152.

Rangaswamy, M, Weiner, D, and Ozturk, A. (1993), Non-Gaussian Random Vector Identification Using Spherically Invariant Random Processes. *IEEE Trans. Aero. Elec. Sys.* Vol. 29, 111-123.

Rosenberg, L., Crisp, D. J. and Stacy, N. J. (2010). Analysis of the KK-Distribution with Medium Grazing Angle Sea Clutter. *IET Radar, Sonar, Navig.* Vol. 4, 209-222.

Schleher, D. C. (1976). Radar Detection in Weibull Clutter. *IEEE Trans. Aero. Elec. Sys.* Vol. AES-12, 736-743.

Shnidman, D. A. (1999). Generalized Radar Clutter Model. *IEEE Trans. Aero. Elec. Sys.* Vol.35, 857-865.

Skolnik, M. (2008). *Introduction to Radar Systems: Third Edition*. McGraw-Hill, New York.

Stacy, N., Badger, D., Goh, A., Preiss, M. and Williams, M. (2003). The DSTO Ingara Airborne X-Band SAR Polarimetric Upgrade: First Results. *IEEE Proceed. Int. Symp. Geo. Remote Sensing (IGARSS)* Vol. 7, 4474-4475.

Stacy, N, Crisp, D., Goh, A., Badger, D. and Preiss, M. (2005). Polarimetric Analysis of Fine Resolution X-Band Sea Clutter Data. *Proc. IGARSS 05*, 2787-2790.

Stimson, G. W. (1988). *Introduction to Airborne Radar: Second Edition*. Scitech Publishing, Inc, Rayleigh, NC.

Trunk, G. V. and George, S. F. (1970). Detection of Targets in Non-Gaussian Sea Clutter. *IEEE Trans. Aero. Elec. Sys.* Vol.AES-6, 620-628.

Valeyrie, N., Garello, R., Quellec, J.-M. and Chabah, M. (2009). Study of the Modeling of Radar Sea Clutter Using the KA-Distribution and Methods for Estimating its Parameters, *Radar Conf: Surveillance for a Safer World*.

Ward, K. D. (1981). Compound Representation of High Resolution Sea Clutter. *IEE Elec. Lett.* Vol. 17, 561-563.

Ward, K. D., Watts. S. and Tough, R. J. A. (2006). *Sea Clutter: Scattering, the K-Distribution and Radar Performance*. IET Radar, Sonar and Nav., Series 20, IET London.

Ward, K. D. and Tough, R. J. A. (2002). Radar Detection Performance in Sea Clutter with Discrete Spikes. *International Radar Conference*, 253-257.

Watts, S., Ward, K. D. and Tough, R. J. A. (2005). The Physics and Modelling of Discrete Spikes in Radar Sea Clutter. *Proceedings of International Radar Conference*.

Wise, G. and Gallagher, N. C.(1978). On Spherically Invariant Random Processes. *IEEE Trans. Info. Theory* Vol. IT-24, 118-120.

Yao, K. (1973). A Representation Theorem and Its Application to Spherically-Invariant Random Processes. *IEEE Trans. Info. Theory* Vol. IT-19, 600-608.

Digital Communication

Edited by Prof. C Palanisamy

All marketing is digital and everyone should have a digital strategy. Everything is going mobile. "The world has never been more social" is the recent talk in the community. Digital Communication is the key enabler of that. Digital information tends to be far more resistant to transmit and interpret errors than information symbolized in an analog medium. This accounts for the clarity of digitally-encoded telephone connections, compact audio disks, and much of the enthusiasm in the engineering community for digital communications technology. A contemporary and comprehensive coverage of the field of digital communication, this book explores modern digital communication techniques. The purpose of this book is to extend and update the knowledge of the reader in the dynamically changing field of digital communication.

How to reference

In order to correctly reference this scholarly work, feel free to copy and paste the following:

INTECH

open science | open minds